Continuum Mechanics and Thermodynamics manuscript No.
(will be inserted by the editor)

The asymptotic homogenization elasticity tensor properties for composites with material discontinuities

Raimondo Penta · Alf Gerisch

Received: date / Accepted: date

Abstract The classical asymptotic homogenization approach for linear elastic composites with discontinuous material properties is considered as a starting point. The sharp length scale separation between the fine periodic structure and the whole material formally leads to anisotropic elastic-type balance equations on the coarse scale, where the arising fourth rank operator is to be computed solving single periodic cell problems on the fine scale. After revisiting the derivation of the problem, which here explicitly points out how the discontinuity in the individual constituents' elastic coefficients translates into stress jump interface conditions for the cell problems, we prove that the gradient of the cell problem solution is minor symmetric and that its cell average is zero. This property holds for perfect interfaces only (i.e. when the elastic displacement is continuous across the composite's interface), and can be used to assess the accuracy of the computed numerical solutions. These facts are further exploited, together with the individual constituents' elastic coefficients and the specific form of the cell problems, to prove a theorem that characterizes the fourth rank operator appearing in the coarse scale elastic-type balance equations as a composite material effective elasticity tensor. We both recover known facts, such as minor and major symmetries and positive definiteness, and establish new facts concerning the Voigt and Reuss bounds. The latter are shown for the first time without assuming any equivalence between coarse and fine scale energies (*Hill's condition*), which, in contrast to the case of representative volume elements, does not identically hold in the context of asymptotic

R. Penta
Departamento de Mecanica de los Medios Continuos y T. Estructuras,
E.T.S. de caminos, canales y puertos, Universidad Politecnica de Madrid,
Calle Profesor Aranguren S/N, 28040, Madrid, Spain.
Tel.: +34-913366659
Fax: +34-913366702
E-mail: raimondo.penta@upm.es

A. Gerisch
AG Numerik und Wissenschaftliches Rechnen
Dolivostr. 15, 64293 Darmstadt, Germany.
Tel.: +49-61511623173
Fax: +49-61511623164
E-mail: gerisch@mathematik.tu-darmstadt.de

homogenization. We conclude with instructive three dimensional numerical simulations of a soft elastic matrix with an embedded cubic stiffer inclusion to show the profile of the physically relevant elastic moduli (Young's and shear moduli) and Poisson's ratio at increasing (up to 100%) inclusion's volume fraction, thus providing a proxy for the design of artificial elastic composites.

Keywords Multiscale homogenization · Composite materials · Hill's condition · Voigt bound · Reuss bound · Anisotropic elasticity

1 Introduction

The study of elastic composites, see, e.g., [7, 22, 23, 26] is motivated by practical engineering applications involving real materials such as wood, geomaterials, and biological tissues, as well as artificial constructs as, for example, polymers, metals, and biomimetic materials. A thorough understanding of the mechanical behavior of composites on the basis of their constituents' properties can enhance the knowledge concerning real world physical scenarios and improve the design of optimized artificial materials with respect to key physical properties, such as stiffness and toughness. However, these materials are in general multiscale in nature and it is virtually impossible to resolve any single interaction among their constituents, both from a computational and from an experimental viewpoint. These issues motivated the development of the so called multiscale *homogenization* techniques, which aim to find an effective constitutive relationship for the composite material as a whole (thus describing it on a *coarse* scale), which is at the same time capable to (at least partially) retain information concerning the individual constituents' arrangement, properties, and interplay occurring on a *fine* scale. According to the existing literature, the most widely exploited techniques to tackle this issue rely on either the average field or the asymptotic homogenization techniques, see, e.g., the review [21], where these two approaches are discussed and compared.

The average field approach is based on an elastic-type constitutive behavior (a priori assumed) for the whole composite, where the effective elasticity tensor linearly relates fine scale stresses and strains averaged on a *representative volume*. This volume should be large enough to statistically represent the whole structure and, at the same time, sufficiently small to enable a computationally feasible approach for the actual computation of the effective elasticity tensor. This can be achieved by performing elastic-type computations on a *representative volume element* (RVE), which, by definition, satisfies *Hill's condition* [17, 18], i.e., the coarse scale energy (which involves the effective elastic properties) equals the average fine scale energy (see, e.g., [14] for a practical application of the RVE technique for cortical bone). Further average field techniques involve the well-known results by Eshelby [12], i.e. the representative volume is identified with an infinite medium equipped with uniform strain condition at infinity (which also satisfies Hill's condition), and the different constituents are modeled as ellipsoidal inclusions; this way, the strain inside the inclusions turns out to be uniform, and further approximations (such as the Mori-Tanaka [27] and self-consistent [19] schemes) can be exploited to compute the effective elastic constants semi-analytically (see, e.g., [42], where these techniques are exploited to compute the mineralized turkey leg tendon elastic constants and validated against experimental data).

The asymptotic homogenization technique (see, for example, [2, 3, 20, 25, 29, 37]) aims to find the effective governing equations for composite materials enforcing the length scale separation between the fine and coarse scales, which are considered as independent spatial variables; multiple scale expansions of the fields is performed to obtain differential conditions which are used, under the assumption of fine scale periodicity, to derive an elastic-type coarse scale problem for the whole composite. The fine scale information is encoded in the homogenized moduli, which are to be computed solving elastic-type partial differential equations on the single periodic cell only once, thus reducing computational complexity.

Here we embrace the classical asymptotic homogenization approach for an elastic composite with discontinuous material properties. We start revisiting the standard results that can be found in [3, 29, 37] to point out explicitly the role of the interface loads which drive nontrivial cell problems solution whenever there are discontinuities in the constituents coefficients. We setup the problem representing explicitly the different domains and both, continuous spatial variations of elastic costants within a single phase and their jump across the interface between two different phases, are separately taken into account. The gradient of the cell problem solution, which is central in the effective elastic coefficients computation, possesses particular features and symmetries which are proved and discussed. The latter are subsequently exploited to demonstrate the set of properties which characterize the homogenized moduli as actual elastic moduli, i.e. minor and major symmetries and positive definiteness, as well as the Voigt [43] and Reuss [36] bounds for the effective elasticity tensor. The aforementioned properties and bounds (including more refined estimates, such as the Hashin and Shtrikman bounds [15] and their generalizations) are well-known to hold whenever the effective elasticity tensor is defined by a linear relationship between the average stress and strain and Hill's condition [17, 18] is satisfied. This condition is fulfilled by definition for RVE and, in general, for any volume portion if uniform traction, displacement, or periodic boundary conditions are applied. In these cases, the elementary Voigt and Reuss bounds can be proved by means of variation arguments (see, e.g. [26] and [7]) or equivalently by average stress and strain theorems (as, for example, in [44]). Whenever asymptotic homogenization is concerned, even though the fine scale periodic cell plays, from a practical viewpoint, the role of a representative volume, Hill's condition is satisfied for leading order quantities only (as previously noted, for example, in [2]), hence the general formalism which would apply in the context of average field techniques (which can be carried out also for periodic composites, as in the last chapter of [7]) does not hold and different strategies are to be developed.

Issues concerning bounds for the effective coefficients arising from asymptotic homogenization of elliptic problems have been investigated to a lesser extent, and mostly rely on the *H-convergence* theory [28]. The latter framework provides general (in particular, periodicity of the fine scale is not a priori assumed) arguments that can be specialized to rigorously prove existence and uniqueness of the asymptotic homogenized solutions via two scale convergence [1], as done in [8] in the context of linear elasticity with periodic fine scale structure. The work [41] represents a first step towards the identification of bounds for the homogenized coefficients arising from scalar, diffusion-type, elliptic problems. The properties of H-convergence are used to bound the homogenized diffusivity tensor by the L^∞ limit of the fine scale diffusion (from above), and by the inverse of the L^∞ limit

of the inverse of the fine scale diffusion (from below)[1]. The work [13] comprises bounds in elasticity derived in the framework of H-convergence. The authors consider composites made of isotropic constituents and explore a number of possible isotropic homogenized limits (i.e. also isotropy of the homogenized elasticity tensor is assumed when bounds are to be identified). For such restricted cases, they derive bounds for the effective shear and bulk moduli and study optimality compared to the Hashin and Shtrikman bounds [15]. These bounds are not derived assuming periodicity and in fact hold for fine scale structures that result in macroscopically isotropic media (for example, multiple layering of isotropic constituents, as highlighted by the authors). In [24] the authors exploit the findings in [13] to derive bounds for the effective elastic energy of macroscopically anisotropic composites made of isotropic and incompressible constituents in terms of their fine scale shear moduli. These previously known bounds in the context of elasticity rely on specific restriction, such as coarse and/or fine scale isotropy, whereas the Voigt and Reuss bounds, which can be interpreted as bounds on the elastic energy as well, though not optimal, are more general, as they involve the (local average) of the possibly anisotropic constituents' elasticity tensors (and their inverse). This generality makes these bounds a paramount characterization of elastic composites in the engineering literature. In [25], the authors develop a variational setting and exploit the cell problem interface conditions directly to prove the aforementioned bounds in the particular case of local oscillations but continuous coefficients at the two-phase elastic composite's interface.

Here, we extend the existing literature for asymptotic homogenization of elastic composites which can possibly exhibit both discontinuos material properties and local oscillations. We present the following results (a-c) below. (a) Rigorous proof of the properties of the auxiliary fourth rank tensor that represents the gradient of the cell problems solution. The necessary role of continuity of displacements across the composite interface is remarked and the latter properties are used to prove crucial properties of the effective elasticity tensor and can be exploited to assess the reliability of fine scale numerical simulations. (b) A theorem that provides alternative, yet equivalent, representations of the effective elasticity tensors, which are exploited to recover its standard minor and major symmetries and positive definiteness properties (in analogy to those proved in the two scale convergence context in [8]) and to prove for the first time the Voigt and Reuss bounds without assuming Hill's condition. (c) Innovative three dimensional simulations (complementary to those reported in [33]), representing the mechanical behavior of a stiff cubic inclusion embedded in a softer matrix to highlight the effective Young's modulus, shear modulus, and Poisson's ratio profiles at inclusion's volume fraction ranging from 0 to 100%.

The paper is organized as follows:

- In Section 2 we present a revisited derivation of the asymptotic homogenization model for linear elastic composites with discontinuous material properties and present a novel theorem concerning key properties of the cell problem solution.
- In Section 3, we embrace a direct, yet rigorous, approach and enforce the individual constituents' elasticity tensor properties and the results proved in Section 2 to prove a theorem that characterizes the fourth rank tensor arising

[1] English translations of the works [28, 41] performed by the authors themselves can be found in chapter 2 and 3 of [7], respectively.

from the asymptotic homogenization approach as a composite material *effective elasticity tensor*, in terms of minor and major symmetries, positive definiteness (recovering previously derived results), and the Voigt and Reuss bounds proved for the first time without assuming the Hill's condition.
- In Section 4 we perform three dimensional numerical tests to predict the mechanical behavior of an elastic composite at increasing volume fraction of the embedded cubic inclusion.
- In Section 5 we present concluding remarks and further perspectives.

2 Asymptotic homogenization and the properties of the cell problems

The classical asymptotic homogenization approach for elastic composites exploits the length scale separation between the fine local structure (where interactions among the individual constituents are clearly resolved) and the whole medium, to derive effective elastic-type balance equations which hold on the *coarse scale*. The homogenized elastic moduli are to be computed solving periodic cell problems on the *fine scale* local structure. The technique has its mathematical foundation in the pioneering works reported in [29] for elliptic problems, which have been extended to the elastic problem in [37], where the extension to discontinuous coefficients is suggested in weak form and formally appears as a volume contribution in the related cell problems. In [3], a general procedure is employed to derive averaged elliptic equations of infinite order of accuracy, which can be used, for example, in the context of strain gradient elasticity as in [30]. Following recent advances in the multiscale asymptotics literature (see, e.g., [31, 32, 39]), we provide a modern and revisited derivation of the problem, which is formally carried out in strong form and points out explicitly the role of volume and boundary loads that appear in the arising periodic cell problem. This introductory background provides us a clear framework to prove for the properties of the periodic cell problems solutions, which are subsequently used in Section 3 to prove our main result concerning the properties of the effective elasticity tensor. We first introduce the standard elastic problem for composites and the basis of asymptotic homogenization. Application of the technique steps leads to the coarse scale problem. Finally, we prove a novel theorem which depicts peculiar properties of the cell problem solutions.

2.1 Formulation of the elastic problem for material composites

We start setting up a linear elastic problem assuming the interaction between a matrix and a number of inclusions [2]. This choice is performed for the sake of simplicity of notation only, as every result proved in the current work is actually valid for an arbitrary number of subphases (i.e. inclusions and fibers) embedded in the host medium, see our computational study reported in [33] for a straightforward generalization of the problem to multiphase linear elastic composites.

[2] We refer to inclusion for simplicity of terminology and to foster the reader's intuition, although the current formulation and related proofs hold also for fiber reinforced composites

We represent the composite as a bounded domain $\Omega \subset \mathbb{R}^3$, such that $\bar{\Omega} = \bar{\Omega}_A \cup \bar{\Omega}_B$, $\Omega_A \cap \Omega_B = \emptyset$. Here, Ω_A represents the host medium (*the matrix*) and

$$\Omega_B = \bigcup_{\alpha=1}^{N} \Omega_{B_\alpha}. \tag{1}$$

a number N of disjoint embedded inclusions Ω_{B_α}. We assume that both the matrix and the inclusions behave as linear elastic materials with constitutive relationships for the stress tensors σ_A and σ_{B_α}

$$\sigma_A = \mathbb{C}^A \nabla \boldsymbol{u}_A, \tag{2}$$

$$\sigma_{B_\alpha} = \mathbb{C}^B \nabla \boldsymbol{u}_{B_\alpha}, \tag{3}$$

where, for every $\boldsymbol{x} \in \Omega$, $\boldsymbol{u}_A(\boldsymbol{x})$ is the restriction of the elastic displacement $\boldsymbol{u}(\boldsymbol{x})$ to Ω_A and $\boldsymbol{u}_{B_\alpha}(\boldsymbol{x})$ denotes the elastic displacement restricted to the inclusion Ω_{B_α}

$$\boldsymbol{u}_A = \boldsymbol{u}|_{\Omega_A}; \quad \boldsymbol{u}_{B_\alpha} = \boldsymbol{u}|_{\Omega_{B_\alpha}}. \tag{4}$$

The fourth rank tensors $\mathbb{C}^A(\boldsymbol{x})$, $\mathbb{C}^B(\boldsymbol{x})$ (with components C^A_{ijkl}, C^B_{ijkl} for $i,j,k,l = 1,2,3$) are the elasticity tensors in Ω_A and Ω_B, respectively. They possess major symmetry

$$C^A_{ijkl} = C^A_{klij};\ C^B_{ijkl} = C^B_{klij} \tag{5}$$

and left and right minor symmetry

$$C^A_{ijkl} = C^A_{jikl};\ C^B_{ijkl} = C^B_{jikl};\ C^A_{ijkl} = C^A_{ijlk};\ C^B_{ijkl} = C^B_{ijlk}, \tag{6}$$

the latter leading to

$$\mathbb{C}^A \nabla \boldsymbol{u}_A = \mathbb{C}^A \xi(\boldsymbol{u}_A);\ \mathbb{C}^B \nabla \boldsymbol{u}_{B_\alpha} = \mathbb{C}^B \xi(\boldsymbol{u}_{B_\alpha}), \tag{7}$$

where

$$\xi(\bullet) = \frac{\nabla(\bullet) + \nabla(\bullet)^{\mathsf{T}}}{2}, \tag{8}$$

i.e. $\xi(\boldsymbol{u}_A)$, $\xi(\boldsymbol{u}_{B_\alpha})$ are the matrix and inclusion elastic strain tensors. We enforce the stress balance equations in Ω_A and in each inclusion in Ω_{B_α} ignoring volume forces and inertia. We close the problem by coupling the matrix and the inclusions via continuity of stresses and displacements across every interface $\Gamma_\alpha := \partial\Omega_A \cap \partial\Omega_{B_\alpha}$ and prescribe proper external boundary conditions on $\partial\Omega$. Therefore, the resulting boundary value problem reads

$$\nabla \cdot \sigma_A = 0 \qquad \text{in } \Omega_A, \tag{9}$$

$$\nabla \cdot \sigma_{B_\alpha} = 0 \qquad \text{in } \Omega_{B_\alpha}, \tag{10}$$

$$\sigma_A \boldsymbol{n}^\alpha = \sigma_{B_\alpha} \boldsymbol{n}^\alpha \qquad \text{on } \Gamma^\alpha, \tag{11}$$

$$\boldsymbol{u}_A = \boldsymbol{u}_{B_\alpha} \qquad \text{on } \Gamma^\alpha, \tag{12}$$

$$+\,\text{boundary conditions} \qquad \text{on } \partial\Omega, \tag{13}$$

for $\alpha = 1...N$. Here, $\boldsymbol{n}^\alpha$ denotes the unit vector in $\boldsymbol{x} \in \Gamma^\alpha$ normal to the interface Γ^α pointing into the inclusion Ω_{B_α} and σ_A, σ_{B_α} are given by the constitutive

relationships (2) and (3), respectively. The elasticity tensors $\mathbb{C}^A$ and $\mathbb{C}^B$ are assumed as smooth functions of $\boldsymbol{x}$ in Ω_A and every Ω_{B_α}, respectively. The material properties are assumed, in general, discontinuous, that is

$$\left(\mathbb{C}^A(\boldsymbol{x}) - \mathbb{C}^B(\boldsymbol{x})\right) \neq \mathsf{0} \text{ on } \Gamma^\alpha. \tag{14}$$

Next, we introduce the asymptotic homogenization technique based on the length scale separation assumption.

2.2 The asymptotic homogenization technique

We consider a typical fine scale d, which characterizes the local structure, and the coarse scale L which represents the size of the whole domain Ω. We then assume that these length scales are well-separated, namely:

$$\frac{d}{L} = \epsilon \ll 1. \tag{15}$$

We enforce spatial scale decoupling exploiting condition (15) to relate d (the *fine scale*) and L (the *coarse scale*) as follows:

$$\boldsymbol{y} := \frac{\boldsymbol{x}}{\epsilon}. \tag{16}$$

From now on $\boldsymbol{x}$ and $\boldsymbol{y}$ denote independent variables, representing the coarse and fine spatial coordinates, respectively. Each field and material property is then assumed to be a function of both the independent spatial variables $\boldsymbol{x}$ and $\boldsymbol{y}$, namely

$$\boldsymbol{u}_A = \boldsymbol{u}_A(\boldsymbol{x}, \boldsymbol{y}),\ \boldsymbol{u}_{B_\alpha} = \boldsymbol{u}_{B_\alpha}(\boldsymbol{x}, \boldsymbol{y}), \tag{17}$$

$$\mathbb{C}^A = \mathbb{C}^A(\boldsymbol{x}, \boldsymbol{y}),\ \mathbb{C}^B = \mathbb{C}^B(\boldsymbol{x}, \boldsymbol{y}). \tag{18}$$

By virtue of the performed spatial scale decoupling, we obtain, by the chain rule, the following transformation for differential operators:

$$\nabla \to \nabla_{\boldsymbol{x}} + \frac{1}{\epsilon}\nabla_{\boldsymbol{y}}. \tag{19}$$

We now assume that the elastic displacement $\boldsymbol{u}$ can be represented by multiscale expansions in powers of ϵ:

$$\boldsymbol{u}^\epsilon(\boldsymbol{x}, \boldsymbol{y}) = \sum_{l=0}^{\infty} \boldsymbol{u}^{(l)}(\boldsymbol{x}, \boldsymbol{y})\epsilon^l. \tag{20}$$

We substitute the power series representation (20) applied to the restrictions $\boldsymbol{u}_A$ and $\boldsymbol{u}_{B_\alpha}$, together with relationship (19), into the system (9-12) and equations (2-3). As a result, multiplying each equation by a suitable power of ϵ and exploiting (7), we obtain the multiscale differential system for the elastic composite, namely

$$\begin{aligned} \nabla_{\boldsymbol{y}} \cdot \left(\mathbb{C}^A \xi_{\boldsymbol{y}}(\boldsymbol{u}_A^\epsilon)\right) + \epsilon \nabla_{\boldsymbol{y}} \cdot \left(\mathbb{C}^A \xi_{\boldsymbol{x}}(\boldsymbol{u}_A^\epsilon)\right) + \\ + \epsilon \nabla_{\boldsymbol{x}} \cdot \left(\mathbb{C}^A \xi_{\boldsymbol{y}}(\boldsymbol{u}_A^\epsilon)\right) + \epsilon^2 \nabla_{\boldsymbol{x}} \cdot \left(\mathbb{C}^A \xi_{\boldsymbol{x}}(\boldsymbol{u}_A^\epsilon)\right) = 0 \quad \text{in } \Omega_A, \end{aligned} \tag{21}$$

$$\begin{aligned}\nabla_{\boldsymbol{y}}\cdot\left(\mathbb{C}^B\xi_{\boldsymbol{y}}(\boldsymbol{u}^\epsilon_{B_\alpha})\right)+\epsilon\nabla_{\boldsymbol{y}}\cdot\left(\mathbb{C}^B\xi_{\boldsymbol{x}}(\boldsymbol{u}^\epsilon_{B_\alpha})\right)+\\ +\epsilon\nabla_{\boldsymbol{x}}\cdot\left(\mathbb{C}^B\xi_{\boldsymbol{y}}(\boldsymbol{u}^\epsilon_{B_\alpha})\right)+\epsilon^2\nabla_{\boldsymbol{x}}\cdot\left(\mathbb{C}^B\xi_{\boldsymbol{x}}(\boldsymbol{u}^\epsilon_{B_\alpha})\right)=0\quad\text{in }\Omega_{B_\alpha},\end{aligned}\tag{22}$$

$$\mathbb{C}^A\xi_{\boldsymbol{y}}(\boldsymbol{u}^\epsilon_A)\boldsymbol{n}^\alpha-\mathbb{C}^B\xi_{\boldsymbol{y}}(\boldsymbol{u}^\epsilon_{B_\alpha})\boldsymbol{n}^\alpha=\epsilon\mathbb{C}^B\xi_{\boldsymbol{x}}(\boldsymbol{u}^\epsilon_{B_\alpha})\boldsymbol{n}^\alpha-\epsilon\mathbb{C}^A\xi_{\boldsymbol{x}}(\boldsymbol{u}^\epsilon_A)\boldsymbol{n}^\alpha\quad\text{on }\Gamma^\alpha,\tag{23}$$

$$\boldsymbol{u}^\epsilon_A=\boldsymbol{u}^\epsilon_{B_\alpha}\quad\text{on }\Gamma^\alpha.\tag{24}$$

We finally assume $\boldsymbol{y}$-periodicity for every field and constituent elasticity tensor. This technical assumption will enable us to retain fine scale geometrical information focusing on a small portion of the local structure only. From now on, we identify the domain Ω with its corresponding periodic cell and Ω_A, Ω_B denote the corresponding matrix and inclusion in the cell, respectively (and thus omit the unnecessary index α). Note that the fine scale length d is now defined as the minimum (linear) periodic cell size which can fully represent the fine scale geometry, see Figure 1.

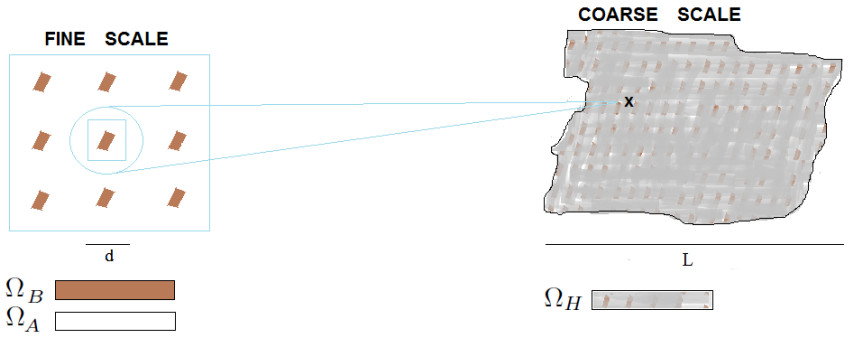

Fig. 1 A 2D schematic representing the fine and coarse scales. On the right hand side, the coarse scale domain, where the fine scale structure is smoothed out, is shown. On the left hand side, a sample periodic unit representing the fine scale is shown and the different between the matrix and the inclusion is clearly resolved.

In the following section, we equate coefficients of ϵ^l for $l=0,1,2,...$ in (21-24) to obtain a homogenized model in terms of the leading (zeroth) order elastic displacement field in the coarse scale domain Ω_H (see Figure 1). Since the quantities involved in the definition of this problem can also vary on the local scale $\boldsymbol{y}$, we define the following *cell average* operators

$$\langle\bullet\rangle=\frac{1}{|\Omega|}\int_\Omega\bullet\,\mathrm{d}\boldsymbol{y};\quad\langle\bullet\rangle_A=\frac{1}{|\Omega|}\int_{\Omega_A}\bullet\,\mathrm{d}\boldsymbol{y};\quad\langle\bullet\rangle_B=\frac{1}{|\Omega|}\int_{\Omega_B}\bullet\,\mathrm{d}\boldsymbol{y},\tag{25}$$

where $|\Omega|$ represents the periodic cell volume.

2.3 The coarse scale model derivation

Equating coefficients of ϵ^0 in (21-24) yields

$$\nabla_{\boldsymbol{y}} \cdot \left(\mathbb{C}^A \xi_{\boldsymbol{y}}(\boldsymbol{u}_A^{(0)}) \right) = 0 \qquad \text{in } \Omega_A, \tag{26}$$

$$\nabla_{\boldsymbol{y}} \cdot \left(\mathbb{C}^B \xi_{\boldsymbol{y}}(\boldsymbol{u}_B^{(0)}) \right) = 0 \qquad \text{in } \Omega_B, \tag{27}$$

$$\mathbb{C}^A \xi_{\boldsymbol{y}}(\boldsymbol{u}_A^{(0)})\boldsymbol{n} = \mathbb{C}^B \xi_{\boldsymbol{y}}(\boldsymbol{u}_B^{(0)})\boldsymbol{n} \qquad \text{on } \Gamma, \tag{28}$$

$$\boldsymbol{u}_A^{(0)} = \boldsymbol{u}_B^{(0)} \qquad \text{on } \Gamma, \tag{29}$$

whereas equating coefficients of ϵ^1 in (21-24) leads to

$$\nabla_{\boldsymbol{y}} \cdot \left(\mathbb{C}^A \xi_{\boldsymbol{y}}(\boldsymbol{u}_A^{(1)}) \right) + \nabla_{\boldsymbol{x}} \cdot \left(\mathbb{C}^A \xi_{\boldsymbol{y}}(\boldsymbol{u}_A^{(0)}) \right) = -\nabla_{\boldsymbol{y}} \cdot \left(\mathbb{C}^A \xi_{\boldsymbol{x}}(\boldsymbol{u}_A^{(0)}) \right) \quad \text{in } \Omega_A, \tag{30}$$

$$\nabla_{\boldsymbol{y}} \cdot \left(\mathbb{C}^B \xi_{\boldsymbol{y}}(\boldsymbol{u}_B^{(1)}) \right) + \nabla_{\boldsymbol{x}} \cdot \left(\mathbb{C}^B \xi_{\boldsymbol{y}}(\boldsymbol{u}_B^{(0)}) \right) = -\nabla_{\boldsymbol{y}} \cdot \left(\mathbb{C}^B \xi_{\boldsymbol{x}}(\boldsymbol{u}_B^{(0)}) \right) \quad \text{in } \Omega_B, \tag{31}$$

$$\mathbb{C}^A \xi_{\boldsymbol{y}}(\boldsymbol{u}_A^{(1)})\boldsymbol{n} - \mathbb{C}^B \xi_{\boldsymbol{y}}(\boldsymbol{u}_B^{(1)})\boldsymbol{n} = \mathbb{C}^B \xi_{\boldsymbol{x}}(\boldsymbol{u}_B^{(0)})\boldsymbol{n} - \mathbb{C}^A \xi_{\boldsymbol{x}}(\boldsymbol{u}_A^{(0)})\boldsymbol{n} \quad \text{on } \Gamma, \tag{32}$$

$$\boldsymbol{u}_A^{(1)} = \boldsymbol{u}_B^{(1)} \quad \text{on } \Gamma. \tag{33}$$

Finally, when equating coefficients of ϵ^2 in (21-23) we obtain

$$\begin{aligned} &\nabla_{\boldsymbol{y}} \cdot \left(\mathbb{C}^c \xi_{\boldsymbol{y}}(\boldsymbol{u}_c^{(2)}) \right) + \nabla_{\boldsymbol{y}} \cdot \left(\mathbb{C}^c \xi_{\boldsymbol{x}}(\boldsymbol{u}_c^{(1)}) \right) + \\ &+ \nabla_{\boldsymbol{x}} \cdot \left(\mathbb{C}^c \xi_{\boldsymbol{y}}(\boldsymbol{u}_c^{(1)}) \right) + \nabla_{\boldsymbol{x}} \cdot \left(\mathbb{C}^c \xi_{\boldsymbol{x}}(\boldsymbol{u}_c^{(0)}) \right) = 0 \quad \text{in } \Omega_c, \end{aligned} \tag{34}$$

$$\begin{aligned} &\nabla_{\boldsymbol{y}} \cdot \left(\mathbb{C}^B \xi_{\boldsymbol{y}}(\boldsymbol{u}_B^{(2)}) \right) + \nabla_{\boldsymbol{y}} \cdot \left(\mathbb{C}^B \xi_{\boldsymbol{x}}(\boldsymbol{u}_B^{(1)}) \right) + \\ &+ \nabla_{\boldsymbol{x}} \cdot \left(\mathbb{C}^B \xi_{\boldsymbol{y}}(\boldsymbol{u}_B^{(1)}) \right) + \nabla_{\boldsymbol{x}} \cdot \left(\mathbb{C}^B \xi_{\boldsymbol{x}}(\boldsymbol{u}_B^{(0)}) \right) = 0 \quad \text{in } \Omega_B, \end{aligned} \tag{35}$$

$$\mathbb{C}^A \xi_{\boldsymbol{y}}(\boldsymbol{u}_A^{(2)})\boldsymbol{n} - \mathbb{C}^B \xi_{\boldsymbol{y}}(\boldsymbol{u}_B^{(2)})\boldsymbol{n} = \mathbb{C}^B \xi_{\boldsymbol{x}}(\boldsymbol{u}_B^{(1)})\boldsymbol{n} - \mathbb{C}^A \xi_{\boldsymbol{x}}(\boldsymbol{u}_A^{(1)})\boldsymbol{n} \quad \text{on } \Gamma. \tag{36}$$

The solutions of the periodic cell problem (26-29) are $\boldsymbol{y}$-constant functions. Hence, since continuity across the interfaces Γ holds, the leading order displacement field reads

$$\boldsymbol{u}^{(0)}(\boldsymbol{x}) = \boldsymbol{u}_A^{(0)}(\boldsymbol{x}) = \boldsymbol{u}_B^{(0)}(\boldsymbol{x}) \tag{37}$$

and we also simplify the notation defining

$$\bar{\boldsymbol{u}}(\boldsymbol{x}) = \boldsymbol{u}^{(0)}(\boldsymbol{x}). \tag{38}$$

Employing relationships (37-38) in equations (30-33), we obtain the following differential problem for the fields $\boldsymbol{u}_A^{(1)}(\boldsymbol{x},\boldsymbol{y})$, $\boldsymbol{u}_B^{(1)}(\boldsymbol{x},\boldsymbol{y})$:

$$\nabla_{\boldsymbol{y}} \cdot \left(\mathbb{C}^A \xi_{\boldsymbol{y}}(\boldsymbol{u}_A^{(1)})\right) = -\nabla_{\boldsymbol{y}} \cdot \left(\mathbb{C}^A \xi_{\boldsymbol{x}}(\bar{\boldsymbol{u}})\right) \quad \text{in } \Omega_A, \tag{39}$$

$$\nabla_{\boldsymbol{y}} \cdot \left(\mathbb{C}^B \xi_{\boldsymbol{y}}(\boldsymbol{u}_B^{(1)})\right) = -\nabla_{\boldsymbol{y}} \cdot \left(\mathbb{C}^B \xi_{\boldsymbol{x}}(\bar{\boldsymbol{u}})\right) \quad \text{in } \Omega_B, \tag{40}$$

$$\mathbb{C}^A \xi_{\boldsymbol{y}}(\boldsymbol{u}_A^{(1)})\boldsymbol{n} - \mathbb{C}^B \xi_{\boldsymbol{y}}(\boldsymbol{u}_B^{(1)})\boldsymbol{n} = \left(\mathbb{C}^B - \mathbb{C}^A\right) \xi_{\boldsymbol{x}}(\bar{\boldsymbol{u}})\boldsymbol{n} \quad \text{on } \Gamma, \tag{41}$$

$$\boldsymbol{u}_A^{(1)} = \boldsymbol{u}_B^{(1)} \quad \text{on } \Gamma. \tag{42}$$

The problem (39-42) is a linear elastic-type periodic boundary value problem equipped with continuity and stress jump interface conditions on Γ. Exploiting linearity, the restrictions $\boldsymbol{u}_A^{(1)}$, $\boldsymbol{u}_B^{(1)}$ to the solution

$$\boldsymbol{u}^{(1)} = \begin{cases} \boldsymbol{u}_A^{(1)} & : \ \boldsymbol{y} \in \ \Omega_A \\ \boldsymbol{u}_B^{(1)} & : \ \boldsymbol{y} \in \ \Omega_B \end{cases}$$

are given by the ansätze

$$\boldsymbol{u}_A^{(1)} = \chi^A \xi_{\boldsymbol{x}}(\bar{\boldsymbol{u}}), \ \boldsymbol{u}_B^{(1)} = \chi^B \xi_{\boldsymbol{x}}(\bar{\boldsymbol{u}}). \tag{43}$$

The third rank tensor χ,

$$\chi = \begin{cases} \chi^A & : \ \boldsymbol{y} \in \ \Omega_A \\ \chi^B & : \ \boldsymbol{y} \in \ \Omega_B, \end{cases} \tag{44}$$

is the solution of the following periodic cell problems:

$$\frac{\partial}{\partial y_j}\left(C^A_{ijpq}\xi^{kl}_{pq}(\chi^A)\right) = -\frac{\partial C^A_{ijkl}}{\partial y_j} \text{ in } \Omega_A, \tag{45}$$

$$\frac{\partial}{\partial y_j}\left(C^B_{ijpq}\xi^{kl}_{pq}(\chi^B)\right) = -\frac{\partial C^B_{ijkl}}{\partial y_j} \text{ in } \Omega_B, \tag{46}$$

$$C^A_{ijpq}\xi^{kl}_{pq}(\chi^A)n^B_j - C^B_{ijpq}\xi^{kl}_{pq}(\chi^B)n^B_j = (C^B - C^A)_{ijkl}n^B_j \text{ on } \Gamma, \tag{47}$$

$$\chi^A_{ikl} = \chi^B_{ikl} \text{ on } \Gamma, \tag{48}$$

where we set

$$\xi^{kl}_{pq}(\chi^A) = \frac{1}{2}\left(\frac{\partial \chi^A_{pkl}}{\partial y_q} + \frac{\partial \chi^A_{qkl}}{\partial y_p}\right); \ \xi^{kl}_{pq}(\chi^B) = \frac{1}{2}\left(\frac{\partial \chi^B_{pkl}}{\partial y_q} + \frac{\partial \chi^B_{qkl}}{\partial y_p}\right) \tag{49}$$

and sum over repeated indices p, q, j is understood. The problem (45-48) is then closed by periodic conditions on $\partial\Omega$, whereas a further condition is to be imposed for uniqueness, for example

$$\left\langle \chi^A_{ikl} \right\rangle_A = \left\langle \chi^B_{ikl} \right\rangle_B = 0 \quad i,k,l = 1,2,3. \tag{50}$$

Remark 1 Note that nontrivial solutions of the cell problems are a direct consequence of both local variations of the elastic constants within the composite constituents, which formally appear as volume forces on the right hand side of (45-46), and of the interface loadings which appear in the stress discontinuity conditions (47). In the latter case, the contribution is directly related to the difference in the elastic constants between the matrix and the inclusion, and to the interface geometry. The interface loadings are nonzero even when the elastic properties are constants within the individual constituent. In this case, these interface loadings are the only driving force for the cell problems (45-48).

We now aim to formulate the effective governing equations for the elastic composite material. We apply the integral average operators (25) over Ω_A and Ω_B in equation (34) and equation (35), respectively. We then sum every resulting contribution and apply the divergence theorem in $\boldsymbol{y}$, such that, rearranging terms, we obtain:

$$\begin{aligned}
&\frac{1}{|\Omega|}\left[\int_\Gamma \mathbb{C}^A\xi_{\boldsymbol{y}}(\boldsymbol{u}_A^{(2)})\boldsymbol{n}\ \mathrm{dS} - \int_\Gamma \mathbb{C}^B\xi_{\boldsymbol{y}}(\boldsymbol{u}_B^{(2)})\boldsymbol{n}\ \mathrm{dS} + \right.\\
&\quad\left. + \int_\Gamma \mathbb{C}^A\xi_{\boldsymbol{x}}(\boldsymbol{u}_A^{(1)})\boldsymbol{n}\ \mathrm{dS} - \int_\Gamma \mathbb{C}^B\xi_{\boldsymbol{x}}(\boldsymbol{u}_B^{(1)})\boldsymbol{n}\ \mathrm{dS}\right] + \\
&\qquad + \frac{1}{|\Omega|}\int_{\Omega_A} \nabla_{\boldsymbol{x}}\cdot\left(\mathbb{C}^A(\xi_{\boldsymbol{y}}(\boldsymbol{u}_A^{(1)}) + \xi_{\boldsymbol{x}}(\bar{\boldsymbol{u}}))\right)\ \mathrm{d}\boldsymbol{y} + \\
&+ \frac{1}{|\Omega|}\left[\int_{\Omega_B} \nabla_{\boldsymbol{x}}\cdot\left(\mathbb{C}^m(\xi_{\boldsymbol{y}}(\boldsymbol{u}_B^{(1)}) + \xi_{\boldsymbol{x}}(\bar{\boldsymbol{u}}))\right)\ \mathrm{d}\boldsymbol{y}\right] = 0,
\end{aligned} \tag{51}$$

where the contributions over the cell boundaries $\partial\Omega$ cancel due to $\boldsymbol{y}$-periodicity. We account for relationship (36), such that also the contributions over the interface Γ in (51) cancel. Finally, we enforce ansätze (43) to deduce the following effective governing equations for every $\boldsymbol{x} \in \Omega_H$, namely

$$\nabla_{\boldsymbol{x}}\cdot\left(\tilde{\mathbb{C}}(\boldsymbol{x})\xi_{\boldsymbol{x}}(\bar{\boldsymbol{u}})\right) = 0. \tag{52}$$

The effective elasticity tensor $\tilde{\mathbb{C}}$ is given by:

$$\tilde{\mathbb{C}} = \left\langle \mathbb{C}^A + \mathbb{C}^A\mathbb{M}^A \right\rangle_A + \left\langle \mathbb{C}^B + \mathbb{C}^B\mathbb{M}^B \right\rangle_B \tag{53}$$

or, componentwise:

$$\tilde{C}_{ijkl} = \left\langle C^A_{ijkl} + C^A_{ijpq}M^A_{pqkl} \right\rangle_A + \left\langle C^B_{ijkl} + C^B_{ijpq}M^B_{pqkl} \right\rangle_B. \tag{54}$$

The auxiliary fourth rank tensors $\mathbb{M}^A$ and $\mathbb{M}^B$ are defined componentwise as:

$$\begin{aligned}
M^A_{pqkl} &= \xi^{kl}_{pq}(\chi^A) = \frac{1}{2}\left(\frac{\partial\chi^A_{pkl}}{\partial y_q} + \frac{\partial\chi^A_{qkl}}{\partial y_p}\right),\\
M^B_{pqkl} &= \xi^{kl}_{pq}(\chi^B) = \frac{1}{2}\left(\frac{\partial\chi^B_{pkl}}{\partial y_q} + \frac{\partial\chi^B_{qkl}}{\partial y_p}\right).
\end{aligned} \tag{55}$$

2.4 Properties of the cell problems solution

The gradient of the cell problem solution possesses specific properties which are summarized in

Theorem 1 (Properties of $\mathbb{M}$) *Let $\mathbb{M}$ be the fourth rank tensor defined by*

$$\mathbb{M} = \begin{cases} \mathbb{M}^A & : \boldsymbol{y} \in \Omega_A \\ \mathbb{M}^B & : \boldsymbol{y} \in \Omega_B, \end{cases} \tag{56}$$

with restrictions $\mathbb{M}^A$, $\mathbb{M}^B$ given by (55)*. Then the following facts hold:*

(i) $\mathbb{M}$ *possesses both left and right minor symmetries.*
(ii) $\langle \mathbb{M} \rangle = 0$.

Proof (i) The tensor $\mathbb{M}$ is left minor symmetric as the restrictions $\mathbb{M}^A$, $\mathbb{M}^B$ are left minor symmetric according to (55). Right minor symmetry of $\mathbb{M}$ is deduced from the cell problems (45-48) employing right minor symmetry of $\mathbb{C}^A$, $\mathbb{C}^B$.

(ii) Since $\mathbb{M}$ is minor symmetric, then also $\langle \mathbb{M} \rangle$ is minor symmetric, hence we only need to prove that for every $\boldsymbol{y}$-constant second rank symmetric tensor A

$$\langle \mathbb{M} \rangle \, \mathsf{A} = \mathsf{0}. \tag{57}$$

Let us set

$$\boldsymbol{v} = \begin{cases} \boldsymbol{v}^A & : \boldsymbol{y} \in \Omega_A \\ \boldsymbol{v}^B & : \boldsymbol{y} \in \Omega_B, \end{cases} \tag{58}$$

$$\boldsymbol{v}^A = \chi^A \mathsf{A}; \quad \boldsymbol{v}^B = \chi^B \mathsf{A}. \tag{59}$$

We can therefore rewrite $\langle \mathbb{M} \rangle \, \mathsf{A}$ by means of definitions (59) and compute

$$\begin{aligned} \langle \mathbb{M} \rangle \, \mathsf{A} = \langle \mathbb{M}\mathsf{A} \rangle &= \left\langle \mathbb{M}^A \mathsf{A} \right\rangle_A + \sum_{\alpha=1}^{N} \left\langle \mathbb{M}^B \mathsf{A} \right\rangle_B = \\ &= \left\langle \xi_{\boldsymbol{y}}(\boldsymbol{v}^A) \right\rangle_A + \sum_{\alpha=1}^{N} \left\langle \xi_{\boldsymbol{y}}(\boldsymbol{v}^B) \right\rangle_B = \\ &= \frac{1}{2|\Omega|} \sum_{\alpha=1}^{N} \int_{\Gamma} (\boldsymbol{v}^A - \boldsymbol{v}^B) \otimes \boldsymbol{n} + \boldsymbol{n} \otimes (\boldsymbol{v}^A - \boldsymbol{v}^B) \, \mathrm{dS} = \mathsf{0}, \end{aligned} \tag{60}$$

where the contributions over the boundary $\partial\Omega$ cancel due to $\boldsymbol{y}$-periodicity and we applied continuity (48) of the third rank tensor χ, which in turn implies continuity of $\boldsymbol{v}$ across the interfaces Γ. Hence

$$\langle \mathbb{M} \rangle = 0 \tag{61}$$

and the proof is complete. □

Remark 2 Note that relationship (61) holds, in a periodic setting, for *perfect interfaces* only, i.e. when the continuity condition (48) is satisfied. In fact, the latter condition is a direct consequence of the continuity of the elastic displacement across the composite interface (12), which implies continuity of the first order elastic displacement (cf. equation (33)) and, in turn, of the third rank tensor χ (cf. equation (43)). In the most general case of interface debonding the quantity $\langle \mathbb{M} \rangle$ is nonzero and depends on the prescribed jump of the elastic displacement across the composite's interface. The property (61) can also be seen as a simple consequence of periodicity when dealing with asymptotic homogenization in a weak formulation setting, provided that jump discontinuities across the interface of the composite are automatically excluded assuming that χ belongs to an appropriate Sobolev space. (A proper example is the space $\mathcal{H}^1_{per}$, introduced through definition (3.48), page 56 of [8]. In the latter book, property (61) is exploited this way in the context of asymptotic homogenization applied to linear elasticity.)

Accounting for the symmetries proven in Theorem 1(i), the cell problem (45-48) stated in terms of three and four rank tensors, corresponds to six elastic-type cell problems, one for each fixed (k, l), $k \geq l$, that can be solved numerically adopting the computational scheme described in [33]. The property proven in Theorem 1 (ii), which will be widely exploited to prove the theorem in the next section, can be also used as a (necessary, but not sufficient) condition to assess the accuracy of the numerical computations of the cell problems, such as those performed in [33, 34].

In the next section we prove a number the properties that characterize $\tilde{\mathbb{C}}$ as the proper coarse scale elasticity tensor, such that the differential model (52) can be regarded as an actual elastic model in the coarse scale domain.

3 The effective elasticity tensor

At this stage, the relationships (52) formally represent the coarse scale stress balance equations of the composite. In fact, applying asymptotic homogenization (17-20) to the stress fields defined by (2-3) we obtain:

$$\sigma^{(0)}_A = \mathbb{C}^A \xi_{\boldsymbol{x}}(\bar{\boldsymbol{u}}) + \mathbb{C}^A \xi_{\boldsymbol{y}}(\boldsymbol{u}^{(1)}_A) = \left(\mathbb{C}^A + \mathbb{C}^A \mathbb{M}^A\right) \xi_{\boldsymbol{x}}(\bar{\boldsymbol{u}}), \tag{62}$$

$$\sigma^{(0)}_B = \mathbb{C}^B \xi_{\boldsymbol{x}}(\bar{\boldsymbol{u}}) + \mathbb{C}^B \xi_{\boldsymbol{y}}(\boldsymbol{u}^{(1)}_B) = \left(\mathbb{C}^B + \mathbb{C}^B \mathbb{M}^B\right) \xi_{\boldsymbol{x}}(\bar{\boldsymbol{u}}), \tag{63}$$

where we exploited (43) and (55). Therefore, defining

$$\sigma^{(0)} = \begin{cases} \sigma^{(0)}_A & : \ \boldsymbol{y} \in \ \Omega_A \\ \sigma^{(0)}_B & : \ \boldsymbol{y} \in \ \Omega_B \end{cases} \tag{64}$$

and exploiting (53) we have

$$\left\langle \sigma^{(0)} \right\rangle = \tilde{\mathbb{C}} \xi_{\boldsymbol{x}}(\bar{\boldsymbol{u}}), \tag{65}$$

i.e. the coarse scale governing equations (52) can be rewritten in terms of the average leading order stress tensor as

$$\nabla_{\boldsymbol{x}} \cdot \left\langle \sigma^{(0)} \right\rangle = 0. \tag{66}$$

Hence, the next step is to prove the properties that characterize $\tilde{\mathbb{C}}$ as an effective *elasticity* tensor, namely minor and major symmetries and positive definiteness, such that (66) and in turn (52) can be considered as the actual coarse scale elastic model. The upper (Voigt) and lower (Reuss) bounds are also provided, and the proof of our main theorem (which includes all the aforementioned facts) merely exploits the interface conditions that characterize the cell problems, the properties of the auxiliary tensor $\mathbb{M}$ (i.e. Theorem 1) and those of the constituents $\mathbb{C}^A$, $\mathbb{C}^B$. We do not enforce the equivalence between coarse scale and fine scale energies (*Hill's condition*) as this does not identically apply, as also remarked at the end of this section.

3.1 Preliminaries and notation

We first introduce the following notation for the sake of convenience:

$$\mathbb{C} = \begin{cases} \mathbb{C}^A & : \boldsymbol{y} \in \ \Omega_A \\ \mathbb{C}^B & : \boldsymbol{y} \in \ \Omega_B, \end{cases} \tag{67}$$

It is also useful to recall the definition of the transpose operator for fourth rank tensors, that is

Definition 1 Let $\mathbb{T}$ be a fourth rank tensor. The transpose of $\mathbb{T}$, denoted $\mathbb{T}^T$, is the unique fourth rank tensor which satisfies

$$\mathsf{A}\mathbb{T}\mathsf{B} = \mathsf{B}\mathbb{T}^T\mathsf{A} \tag{68}$$

for all second rank tensors A, B. In particular, for any tensor $\mathbb{T}$ with components $T_{ijkl},\ i,j,k,l = 1,2,3$, the componentwise representation of $\mathbb{T}^T$ reads

$$T_{klij}, \tag{69}$$

that is, $\mathbb{T} = \mathbb{T}^T$ if and only if $\mathbb{T}$ has major symmetry. Applying the componentwise representation (69) to two fourth order tensors $\mathbb{T}$ and $\mathbb{S}$, we also obtain

$$(\mathbb{T}\mathbb{S})^T = \mathbb{S}^T\mathbb{T}^T. \tag{70}$$

We further notice that, whenever $\mathbb{T}$ is major symmetric, then for every fourth rank tensor $\mathbb{A}$ we have

$$\left(\mathbb{A}^T\mathbb{T}\mathbb{A}\right)^T = \left(\mathbb{A}^T\left(\mathbb{A}^T\mathbb{T}\right)^T\right) = \mathbb{A}^T\mathbb{T}^T\mathbb{A} = \mathbb{A}^T\mathbb{T}\mathbb{A}, \tag{71}$$

i.e. $\mathbb{A}^T\mathbb{T}\mathbb{A}$ is also major symmetric.

We also recall the definition of positive (semi) definiteness (restricted to fourth rank minor symmetric tensors), that is

Definition 2 A fourth rank minor symmetric tensor $\mathbb{T}$ is called positive semidefinite if for any symmetric second rank tensor A,

$$\mathsf{A}\mathbb{T}\mathsf{A} \geq 0. \tag{72}$$

A fourth rank minor symmetric tensor $\mathbb{T}$ is called positive definite if for any non zero symmetric second rank tensor A

$$\mathsf{A}\mathbb{T}\mathsf{A} > 0. \tag{73}$$

In particular, we point out that positive definiteness of $\mathbb{T}$ also implies the existence of a positive definite inverse $\mathbb{T}^{-1}$ which fulfills

$$\mathbb{T}\mathbb{T}^{-1} = \mathbb{I}, \tag{74}$$

where $\mathbb{I}$ denotes the fourth rank identity tensor satisfying

$$\mathbb{I}\mathsf{A} = \mathsf{A} \tag{75}$$

for every second rank tensor A.

We first prove the following

Lemma 1 *Let $\mathbb{T}$ be a positive definite fourth rank tensor with minor and major symmetries. Then, for all second rank tensors A and B, the following inequality holds:*

$$\frac{1}{2}\left(\mathsf{A}\mathbb{T}\mathsf{A} + \mathsf{B}\mathbb{T}^{-1}\mathsf{B}\right) \geq \mathsf{A}\mathsf{B}, \tag{76}$$

where $\mathsf{A}\mathsf{B}$ denotes the inner product between second rank tensors defined by

$$\mathsf{A}\mathsf{B} = \mathsf{B}\mathsf{A} = A_{ij}B_{ij}, \tag{77}$$

where summation over repeated indices i, j is understood.

Proof We set

$$\mathsf{G} = \mathsf{A} - \mathbb{T}^{-1}\mathsf{B} \tag{78}$$

and compute

$$\begin{aligned}
&\frac{1}{2}\left(\mathsf{A}\mathbb{T}\mathsf{A} + \mathsf{B}\mathbb{T}^{-1}\mathsf{B}\right) = \\
&= \frac{1}{2}\left[\mathsf{G}\mathbb{T}\mathsf{G} + (\mathbb{T}^{-1}\mathsf{B})\mathbb{T}(\mathbb{T}^{-1}\mathsf{B}) + (\mathbb{T}^{-1}\mathsf{B})\mathbb{T}\mathsf{G} + \mathsf{G}\mathbb{T}(\mathbb{T}^{-1}\mathsf{B}) + \mathsf{B}\mathbb{T}^{-1}\mathsf{B}\right] = \\
&= \frac{1}{2}\left(\mathsf{G}\mathbb{T}\mathsf{G} + 2\mathsf{G}\mathsf{B} + 2\mathsf{B}\mathbb{T}^{-1}\mathsf{B}\right) = \frac{1}{2}\left(\mathsf{G}\mathbb{T}\mathsf{G} + 2\mathsf{A}\mathsf{B}\right),
\end{aligned} \tag{79}$$

where we exploited major symmetry of $\mathbb{T}$ to obtain $(\mathbb{T}^{-1}\mathsf{B})\mathbb{T}\mathsf{G} = \mathsf{G}\mathbb{T}(\mathbb{T}^{-1}\mathsf{B}) = \mathsf{G}\mathsf{B}$. Since $\mathbb{T}$ is positive definite

$$\mathsf{G}\mathbb{T}\mathsf{G} \geq 0,$$

thus (79) implies (76). □

3.2 Properties of the effective elasticity tensor

We are now ready to state the theorem that fully characterizes $\tilde{\mathbb{C}}$ as an effective elasticity tensor for the composite material. We first merely use the properties of (a) the auxiliary tensor $\mathbb{M}$ (proved in Theorem 1), (b) the constituents' elasticity tensor $\mathbb{C}$, and (c) the specific form of the cell problems (45-48) to show equivalent representation [3] of $\tilde{\mathbb{C}}$ (point (i)), that are exploited to prove minor and major symmetries (point (ii)) and positive definiteness (point (iii)), thus recovering known facts (see, e.g., [8]). The points (iv) and (v) are entirely novel, and concern the Voigt and Reuss bounds.

[3] The representation $\tilde{\mathbb{C}} = \left\langle (\mathbb{I} + \mathbb{M})^T \mathbb{C} (\mathbb{I} + \mathbb{M}) \right\rangle$ shown here can also be found, although proved using a different approach, in [8], page 198, proposition 10.12

Theorem 2 (Properties of $\tilde{\mathbb{C}}$) *Let us consider the fourth rank tensor $\tilde{\mathbb{C}}$ given by relationship* (53)*. Then, the following facts hold:*

(i) $\tilde{\mathbb{C}}$ *has the following equivalent representations*

$$\tilde{\mathbb{C}} = \langle \mathbb{C} \rangle + \langle \mathbb{C}\mathbb{M} \rangle = \left\langle (\mathbb{I} + \mathbb{M})^T \, \mathbb{C} \, (\mathbb{I} + \mathbb{M}) \right\rangle = \langle \mathbb{C} \rangle - \left\langle \mathbb{M}^T \mathbb{C}\mathbb{M} \right\rangle .$$

(ii) $\tilde{\mathbb{C}}$ *possesses minor and major symmetries.*
(iii) $\tilde{\mathbb{C}}$ *is positive definite.*
(iv) $\langle \mathbb{C} \rangle - \tilde{\mathbb{C}}$ *is positive semidefinite.*
(v) $\tilde{\mathbb{C}} - \left\langle \mathbb{C}^{-1} \right\rangle^{-1}$ *is positive semidefinite.*

Proof (i) We account for relationship (53), such that, exploiting notation (67) and global integral average (25), we immediately obtain

$$\tilde{\mathbb{C}} = \langle \mathbb{C} \rangle + \langle \mathbb{C}\mathbb{M} \rangle . \tag{80}$$

We multiply equation (45) and equations (46) by χ^A_{irs}, χ^B_{irs} and integrate over Ω_A, Ω_B, respectively. Then, summing up the resulting equations and integrating by parts yields:

$$\begin{aligned} \int_{\Omega_A} C^A_{ijpq} \xi^{kl}_{pq}(\chi^A) \xi^{rs}_{ij}(\chi^A) \, \mathrm{d}\boldsymbol{y} + \sum_{\alpha=1}^{N} \int_{\Omega_B} C^B_{ijpq} \xi^{kl}_{pq}(\chi^B) \xi^{rs}_{ij}(\chi^B) \, \mathrm{d}\boldsymbol{y} + \\ + \left[\int_{\Gamma} C^B_{ijpq} \xi^{kl}_{pq}(\chi^B) \chi^B_{irs} n_j \, \mathrm{dS} - \int_{\Gamma} C^A_{ijpq} \xi^{kl}_{pq}(\chi^A) \chi^A_{irs} n_j \, \mathrm{dS} + \right. \\ \left. + \int_{\Gamma} C^B_{ijkl} \chi^B_{irs} n_j \, \mathrm{dS} - \int_{\Gamma} C^A_{ijkl} \chi^A_{irs} n_j \, \mathrm{dS} \right] + \\ + \int_{\Omega_A} C^A_{ijkl} \xi^{rs}_{ij}(\chi^A) \, \mathrm{d}\boldsymbol{y} + \int_{\Omega_B} C^B_{ijkl} \xi^{rs}_{ij}(\chi^B) \, \mathrm{d}\boldsymbol{y} = 0, \end{aligned} \tag{81}$$

where the contributions on $\partial\Omega$ cancel due to $\boldsymbol{y}$-periodicity and summation over repeated indices i, j, p, q is understood. Exploiting interface conditions (47-48), also the contributions over every interface Γ^α in equation (81) cancel, such that, accounting for definitions (55), (56), (25), we obtain

$$\left\langle \mathbb{M}^T \mathbb{C}\mathbb{M} \right\rangle + \left\langle \mathbb{M}^T \mathbb{C} \right\rangle = 0, \tag{82}$$

thus, summing (82) to (80) yields

$$\tilde{\mathbb{C}} = \left\langle (\mathbb{I} + \mathbb{M})^T \, \mathbb{C} \, (\mathbb{I} + \mathbb{M}) \right\rangle . \tag{83}$$

Finally, exploiting major symmetry of $\mathbb{C}$, and property (71), we deduce that $\mathbb{M}^T \mathbb{C}\mathbb{M}$ and hence also $\langle \mathbb{M}^T \mathbb{C}\mathbb{M} \rangle$ is major symmetric. Accounting for relationship (82), $\langle \mathbb{M}^T \mathbb{C} \rangle$ is then major symmetric and

$$\left\langle \mathbb{M}^T \mathbb{C} \right\rangle = \left\langle \mathbb{M}^T \mathbb{C} \right\rangle^T = \left\langle \left(\mathbb{M}^T \mathbb{C} \right)^T \right\rangle = \left\langle \mathbb{C}^T \mathbb{M} \right\rangle = \langle \mathbb{C}\mathbb{M} \rangle . \tag{84}$$

Thus, according to (82) and (84)

$$\langle \mathbb{C}\mathbb{M} \rangle = - \left\langle \mathbb{M}^T \mathbb{C}\mathbb{M} \right\rangle , \tag{85}$$

that is, enforcing representation (80)

$$\tilde{\mathbb{C}} = \langle \mathbb{C} \rangle - \left\langle \mathbb{M}^T \mathbb{C} \mathbb{M} \right\rangle, \tag{86}$$

such that $\tilde{\mathbb{C}}$ possesses the three representations (80), (83) and (86).

(ii) Since $\mathbb{C}$ is major symmetric, then exploiting representation (83), $\tilde{\mathbb{C}}$ is major symmetric via property (71). In order to prove minor symmetries, exploiting representation (80), we only need to prove that $\langle \mathbb{C}\mathbb{M} \rangle$ possesses minor symmetries. This is the case because $\mathbb{C}\mathbb{M}$ is both left and right minor symmetric due to left minor symmetry of $\mathbb{C}$ and right minor symmetry of $\mathbb{M}$, respectively.

(iii) Accounting for positive definiteness of $\mathbb{C}$ and representation (83) we have, for every $\boldsymbol{y}$-constant, second rank symmetric tensor A:

$$\mathsf{A}(\tilde{\mathbb{C}}\mathsf{A}) = \langle \mathsf{B}\,(\mathbb{C}\mathsf{B}) \rangle \geq 0, \tag{87}$$

where we set

$$\mathsf{B} = (\mathbb{I} + \mathbb{M})\mathsf{A}. \tag{88}$$

It follows that $\mathsf{A}(\tilde{\mathbb{C}}\mathsf{A}) = 0$ if and only if $\mathsf{B} = 0$. To prove positive definiteness of $\tilde{\mathbb{C}}$, we therefore only need to prove that

$$\mathsf{B} = 0 \Leftrightarrow \mathsf{A} = \mathsf{0}. \tag{89}$$

Obviously, $\mathsf{A} = \mathsf{0}$ implies $\mathsf{B} = 0$. Let us then assume $\mathsf{B} = (\mathbb{I} + \mathbb{M})\mathsf{A} = \mathsf{0}$, then, enforcing (61) we have

$$0 = \langle (\mathbb{I} + \mathbb{M}) \rangle\, \mathsf{A} = \mathsf{A}, \tag{90}$$

which completes the proof of statement (iii).

(iv) Given a $\boldsymbol{y}$-constant second rank symmetric tensor A, we set

$$\mathsf{D} = \mathbb{M}\mathsf{A}.$$

Exploiting representation (86) yields

$$\mathsf{A}(\langle \mathbb{C} \rangle - \tilde{\mathbb{C}})\mathsf{A} = \left\langle \mathsf{A}(\mathbb{M}^T \mathbb{C} \mathbb{M})\mathsf{A} \right\rangle = \langle \mathsf{D}\mathbb{C}\mathsf{D} \rangle \geq 0, \tag{91}$$

where we enforced positive definiteness of the elasticity tensor $\mathbb{C}$ on the right hand side.

(v) We choose a $\boldsymbol{y}$-constant symmetric second rank D, such that, by means of (83), we obtain

$$\frac{1}{2}\mathsf{D}\tilde{\mathbb{C}}\mathsf{D} = \frac{1}{2} \langle (\mathbb{M}\mathsf{D} + \mathsf{D})\mathbb{C}(\mathbb{M}\mathsf{D} + \mathsf{D}) \rangle\,. \tag{92}$$

We apply inequality (76) to the right hand side of (92) exploiting the following identifications

$$\mathbb{T} = \mathbb{C}; \quad \mathsf{A} = \mathbb{M}\mathsf{D} + \mathsf{D}; \quad \mathsf{B} = \tilde{\mathbb{C}}\mathsf{D} \tag{93}$$

such that

$$\frac{1}{2}\mathsf{D}\tilde{\mathbb{C}}\mathsf{D} \geq \left\langle (\mathbb{M}\mathsf{D} + \mathsf{D})\tilde{\mathbb{C}}\mathsf{D} \right\rangle - \frac{1}{2} \left\langle \mathsf{B}\mathbb{C}^{-1}\mathsf{B} \right\rangle \tag{94}$$

Since $\tilde{\mathbb{C}}$ and D are $\boldsymbol{y}$-constant, exploiting (61) yields

$$\left\langle (\mathbb{M}\mathsf{D} + \mathsf{D})\tilde{\mathbb{C}}\mathsf{D} \right\rangle = \mathsf{D}\tilde{\mathbb{C}}\mathsf{D}, \tag{95}$$

thus substituting (95) in (94), and rearranging terms we obtain

$$\mathsf{D}\tilde{\mathbb{C}}\mathsf{D} = \mathsf{B}\tilde{\mathbb{C}}^{-1}\mathsf{B} \leq \mathsf{B}\left\langle \mathbb{C}^{-1} \right\rangle \mathsf{B} \tag{96}$$

or, equivalently

$$\mathsf{B}\left(\tilde{\mathbb{C}} - \left\langle \mathbb{C}^{-1} \right\rangle^{-1}\right)\mathsf{B} \geq \mathsf{0}, \tag{97}$$

which proves positive semidefiniteness of $\tilde{\mathbb{C}} - \left\langle \mathbb{C}^{-1} \right\rangle^{-1}$ as D was arbitrarily chosen and hence B is also an arbitrary symmetric second rank tensor, due to the positive definiteness and symmetric properties of $\tilde{\mathbb{C}}$. □

Theorem 2 demonstrates that the homogenized tensor $\tilde{\mathbb{C}}$ arising in the effective balance equations (52) satisfies the standard symmetries and positive definiteness property which characterize an actual elasticity tensor. The coarse scale elastic energy density reads

$$W(\xi_{\boldsymbol{x}}(\bar{\boldsymbol{u}})) = \frac{1}{2}\xi_{\boldsymbol{x}}(\bar{\boldsymbol{u}})\tilde{\mathbb{C}}\xi_{\boldsymbol{x}}(\bar{\boldsymbol{u}}) \geq 0. \tag{98}$$

and the problem (52) can now be regarded as the coarse scale *elastic* problem.

Remark 3 Note that, according to Theorem 2, the effective $\tilde{\mathbb{C}}$ is equipped with the so called Voigt (upper) and Reuss (lower) bounds provided by the arithmetic and geometric averages $\langle \mathbb{C} \rangle$ and $\left\langle \mathbb{C}^{-1} \right\rangle^{-1}$, respectively. As we remarked in the introduction, these bounds can be proved to characterize any elasticity tensor $\mathbb{C}^*$ defined on a volume element Ω_R by the relationship:

$$\langle \sigma \rangle_R = \mathbb{C}^* \langle \xi \rangle_R , \tag{99}$$

provided that the so called Hill's condition (see, e.g. [16]) is satisfied, that is

$$\langle \sigma \rangle_R \langle \xi \rangle_R = \langle \sigma \xi \rangle_R , \tag{100}$$

i.e. the coarse scale energy equals the average of the fine scale energy. Here, σ and ξ denote the stress and strain of the material and the integral average is performed over the representative volume element Ω_R (see, e.g [44]). In our context, relationships of the type (99-100) hold for leading order quantities only (when considering equation (65)), therefore Hill's condition is not identically satisfied. In general, when dealing with asymptotic homogenization for multiphase elastic composites, it is necessary to exploit the cell problems properties directly, using either a direct approach (as in the current work) or by means of a variational setting (as in [25], where several of the above properties are proved, in contrast to the work here, assuming continuity of the elastic properties at the composite interface).

In the next section we perform a numerical test to show the qualitative and quantitative profile of the elastic Young's and shear moduli, as well as the Poisson's ratio, obtained applying asymptotic homogenization to a single cubic inclusion problem.

4 Numerical tests

In this section we compute the effective elasticity tensor that is obtained applying asymptotic homogenization to a linear elastic composite made of identical cubic inclusion. We numerically solve the elastic-type cell problems (45-48) to compute the auxiliary tensors $\mathbb{M}^A$ and $\mathbb{M}^B$ defined in (55) and the effective elasticity tensor $\tilde{\mathbb{C}}$ by means of (53). We perform the three dimensional numerical simulations via the finite element software COMSOL Multiphysics and exploit the same computational setting described in detail in [33], in particular assuming a linear elastic isotropic and uniform behavior of both the matrix and the inclusion phases. The Young's moduli and Poisson's ratios, denoted by E_A, E_B and ν_A, ν_B, respectively, are consistent to those exploited in [33]; they refer to the realistic scenario reported in [42], so that, identifying our matrix Ω_A and our inclusion Ω_B with the collagen matrix and the (hydroxyapatite) mineral inclusion in the bone, we have

$$E_A = 5\,[\text{GPa}];\ \nu_A = 0.3;\ E_B = 110\,[\text{GPa}];\ \nu_B = 0.28. \tag{101}$$

The considered geometry possesses three orthogonal planes of symmetry and is invariant with respect to permutation of the three orthogonal axis (see, e.g., [40]). Hence, adopting (from now on) the *Voigt* notation (see e.g. [9]) the elasticity tensor $\tilde{\mathbb{C}}$ is represented by a 6×6 symmetric matrix equipped with *cubic* symmetry (see, e.g. [11]), namely

$$\tilde{\mathbb{C}} = \begin{bmatrix} \tilde{C}_{11} & \tilde{C}_{12} & \tilde{C}_{12} & 0 & 0 & 0 \\ \tilde{C}_{12} & \tilde{C}_{11} & \tilde{C}_{12} & 0 & 0 & 0 \\ \tilde{C}_{12} & \tilde{C}_{12} & \tilde{C}_{11} & 0 & 0 & 0 \\ 0 & 0 & 0 & \tilde{C}_{44} & 0 & 0 \\ 0 & 0 & 0 & 0 & \tilde{C}_{44} & 0 \\ 0 & 0 & 0 & 0 & 0 & \tilde{C}_{44} \end{bmatrix}, \tag{102}$$

that is, three independent elastic parameters fully specify the elastic behavior of the composite. In particular, the homogenized Young's modulus E_H, shear modulus μ_H and Poisson's ratio ν_H read (see, e.g.[4]):

$$E_H = \tilde{C}_{11} - \frac{2\tilde{C}_{12}^2}{\tilde{C}_{11} + \tilde{C}_{12}}; \quad \nu_H = \frac{\tilde{C}_{12}}{\tilde{C}_{11} + \tilde{C}_{12}}; \quad \mu_H = \tilde{C}_{44}. \tag{103}$$

Next, we present a parametric study by varying the volume fraction of the inclusion

$$\phi_m = \frac{|\Omega_B|}{|\Omega|}. \tag{104}$$

We present the results in terms of the Young's modulus E_H, Poisson's ratio ν_H, shear modulus μ_H, and quantifying the deviation of the results from a purely isotropic elastic material for

$$0 < \phi_m < 1,$$

approaching 100% volume fraction at a resolution of 1%.

4.1 Young's and shear elastic moduli

The Young's and shear moduli versus the inclusion volume fraction ϕ_m are reported in Figures 2 and 3, respectively. The elastic moduli are both bounded by their Reuss and Voigt counterparts. This is intuitive, as the bounds proven in Section 3 can be interpreted as energetic bounds and hold for any kind of specific deformation, including those induced by uniaxial and shear loading, represented by the Young's and shear moduli. This argument can be proven applying the Reuss and Voigt bounds and positive definiteness presented in Section 3 to suitable linear combinations of the constant strains A (in Voigt notation):

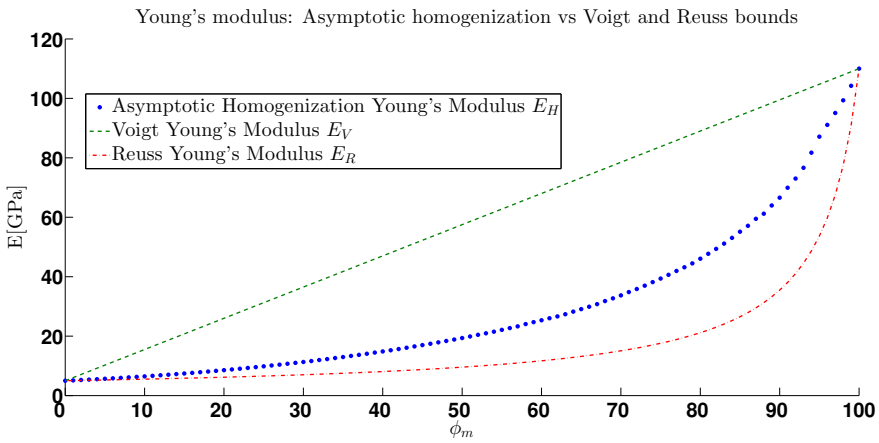

Fig. 2 The asymptotic homogenization Young's modulus E_H, together with the corresponding Voigt and Reuss Young's moduli, is shown as a function of the single cubic inclusion volume fraction ϕ_m.

$$\begin{pmatrix}1\\0\\0\\0\\0\\0\end{pmatrix}, \begin{pmatrix}0\\1\\0\\0\\0\\0\end{pmatrix}, \begin{pmatrix}0\\0\\0\\1\\0\\0\end{pmatrix} \tag{105}$$

leading, for instance, to the following bounds

$$0 < C_{11}^R < \tilde{C}_{11} < C_{11}^V, \tag{106}$$

$$0 < C_{11}^R + C_{12}^R < \tilde{C}_{11} + \tilde{C}_{12} < C_{11}^V + C_{12}^V, \tag{107}$$

and

$$0 < C_{44}^R < \tilde{C}_{44} < C_{44}^V, \tag{108}$$

respectively. Relationships of the kind (106-107) and (108), when applied to definitions (103), finally lead the Voigt and Reuss bounds for the Young's and shear moduli

$$E_R < E_H < E_V, \quad \mu_R < \mu_H < \mu_V, \tag{109}$$

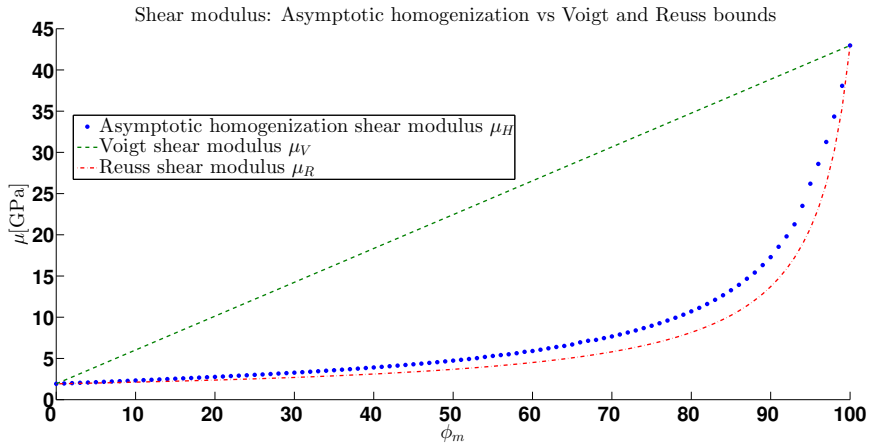

Fig. 3 The asymptotic homogenization shear modulus μ_H, together with the corresponding Voigt and Reuss shear moduli, is shown as a function of the single cubic inclusion volume fraction ϕ_m.

respectively. Our numerical results show for the first time the asymptotic homogenization profile of the Young's and shear moduli for inclusions volume fraction approaching 100%. Although the results hold for a particular geometrical setting, we believe that this study can be used as a first step towards the optimal design of artificial composite materials. The presence of a surrounding soft matrix greatly inhibits the overall material stiffness and we predict that composite remains relatively compliant also for high inclusions volume fraction. This feature (which is also in qualitative agreement with the results obtained via average field techniques, see our computational study [33] for a detailed comparison) can be exploited to obtain composite materials compliant with respect to uniaxial and shear loadings, nonetheless being primarily made of a dramatically stiffer material, which might be useful to maximize other physical properties (such as thermal conductivity and corrosion resistance, etc.).

4.2 Poisson's ratio

The homogenized Poisson's ratio ν_H versus the inclusion volume fraction ϕ_m is shown in Figure 4. The Poisson's ratio does not represent a particular deformation, rather, it is physically defined as the opposite of the ratio of transverse to uniaxial strain, i.e., it is related to the transverse compression of the material at fixed uniaxial loading. Therefore, no bounds apply in this case, and its value can be dramatically lower than that of the individual constituents. This effect can be explained observing that the inclusions within the composite represent a stiff core which inhibits compression in the transverse direction upon uniaxial loading. This peculiar behavior is also captured by Eshelby based technique (although quantitative smaller, see [33]) and RVE techniques, see the computational study reported in [38] for sphere reinforced composites.

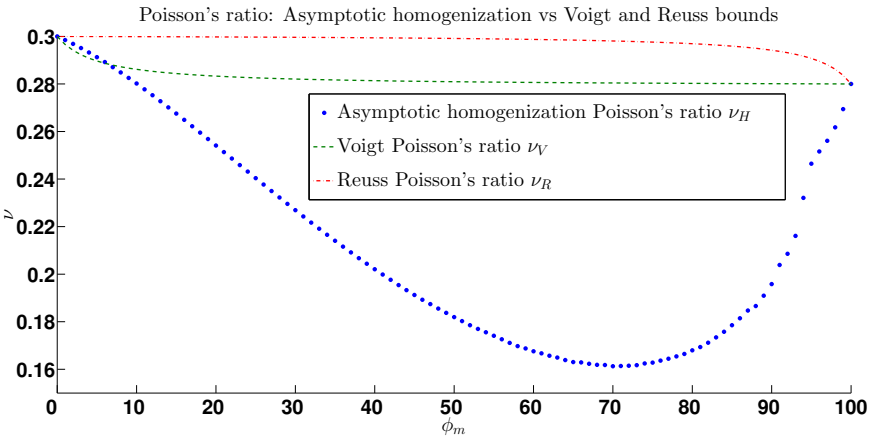

Fig. 4 The asymptotic homogenization Poisson's ratio ν_H, together with the corresponding Voigt and Reuss Poisson's ratios, is shown as a function of the single cubic inclusion volume fraction ϕ_m.

4.3 Deviation from isotropy

The obtained material is anisotropic and cubic symmetric, and the deviation from isotropy can be quantified defining a function DEV as follows:

$$\text{DEV} = \tilde{C}_{11} - (\tilde{C}_{12} + 2\tilde{C}_{44}). \tag{110}$$

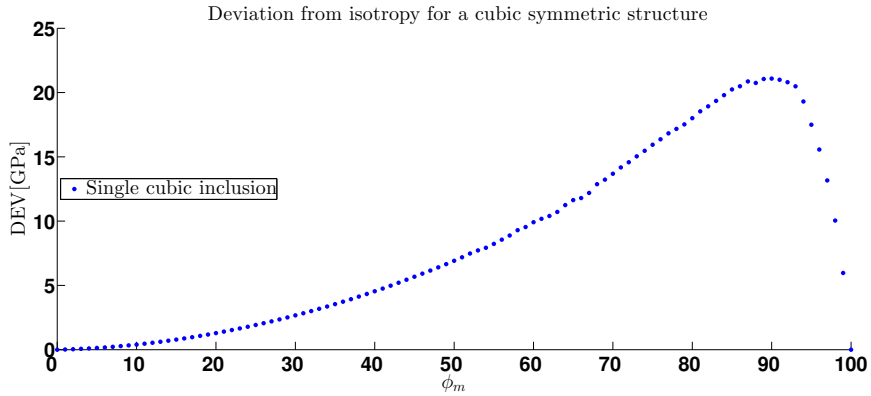

Fig. 5 The deviation from isotropy is shown as a function of the inclusion volume fraction ϕ_m for a single cubic inclusion in a cubic cell.

Whenever DEV $= 0$, relationships (103) turn into the classical definition of the Young's modulus and Poisson's ratio in terms of the shear modulus μ_H and Lamé constant λ_H, i.e.

$$E_H = \frac{\mu_H(3\lambda_H + 2\mu_H)}{\lambda_H + \mu_H}; \quad \nu_H = \frac{\lambda_H}{2(\lambda_H + 2\mu_H)}, \tag{111}$$

where $\tilde{C}_{12}$ is identified with λ_H in the case of isotropy. The nonlinear profile of the deviation from isotropy is shown in Figure 5. Although the individual constituents are isotropic, we obtain an anisotropic, cubic symmetric elasticity tensor. This effect is not merely related to the particular geometrical setting we investigated, rather, it accounts for the prescribed structural arrangement of the inclusions within the matrix. In fact, as highlighted in [33], a cubic symmetric structure is obtained also for spherical inclusions, and the anisotropy that arises from asymptotic homogenization of isotropic constituents is, unlike Eshelby based techniques, not only related to the inclusions aspect ratios.

5 Concluding remarks

We have started from a revisited asymptotic homogenization model for linear elastic composites with discontinuous material properties. Our formulation explicitly highlights how the discontinuity in the individual constituents' elastic coefficients plays a role in the computation of the effective elasticity tensor. The jump in the elastic coefficients across the interface between the matrix and the inclusion translates into stress discontinuity interface conditions in the relevant cell problems. The latter play, in turn, a major role in determining the effective elasticity tensor. The properties reported in Theorem 1 have been exploited to prove our major results concerning the characterization of the fourth rank operator obtained via asymptotic homogenization as the *effective elasticity tensor*, as reported in Section 3. We have proven every property which characterize an elasticity tensor for material composites, that is, major and minor symmetries, positive definiteness, and the energetic lower (Reuss) and upper (Voigt) bounds. We have carried out the proof without considering the periodic cell as an RVE, as it does not fulfill the Hill's condition (the average fine scale energy is not identically equal to the coarse scale energy). We have finally shown a numerical test solving the cell problems for a stiff single cubic inclusion embedded in a softer matrix. We have varied the inclusion volume fraction and presented the results in terms of Young modulus, shear modulus, Poisson's ratio, and deviation from isotropy. We have provided quantitative insights towards the application of asymptotic homogenization for the study of real material composites, complementing the computational analysis reported in [33] on the potential of the technique, and for its application for the optimized design of artificial composites.

The coarse scale model for elastic composites is open to improvement towards a better understanding of real, imperfect, and non periodic elastic composites. We comment on these aspects below.

Our major results reported in Section 3 are only valid whenever Theorem 2 holds, the latter requiring, in turn, perfect interface bonding. In fact, continuity of displacements across the interface translates into a corresponding continuity of the auxiliary displacements in the cell problems, which represents a necessary interface condition to prove that the cell average of the solutions gradient vanishes (see Theorem 1). The present model could be significantly extended to include imperfect interfaces (*interface debonding*), as done for Eshelby based techniques in [35]. The theoretical framework we have developed can be adapted to prove novel bounds (that will in general differ from the standard Voigt and Reuss bounds

proven here) for the effective elastic constants as a function of the specific interface debonding prescription dictated by the actual physical system at hand.

Periodicity of the fine scale geometry is typically assumed when deriving coarse scale models via asymptotic homogenization. Note that this assumption is not strictly necessary to formally derive the coarse scale model as such (see for example the classical derivation of poroelasticity equations carried out in [6] assuming local boundedness only). However, the representative periodic cell enables us to retain fine scale information on the coarse scale, without resolving every geometrical detail of the composite, which is indeed the primary goal of this approach. Following the approach recently developed in [31, 32], it is also possible to generalize the current formulation to non macroscopically uniform media, i.e. retaining fine scale periodicity and allowing for coarse scale variations of the fine scale structure. In this case, the solution of a different cell problem at every coarse scale point would be required, thus greatly affecting the computational cost. High performance parallel computing would be then necessary to solve the cell problems via independent instances, thus reducing the global computational time. In [5, 10], it is also shown how to bypass this issue for specific geometrical setting (including, for example, a collection of spherical obstacles) in the context of advection-diffusion and porous media flow problems.

Finally, although this paper focuses mostly on theoretical aspects, its natural development resides in the application to realistic experimental scenarios (such as musculoskeletal mineralized tissues) and in the optimal design of artificial composite materials. Our results confirm that the computational procedure adopted in [33] has a robust theoretical foundation. Computations based on real composite geometries will allow model validation through comparison against experimental data, and the provided information concerning the mechanical behavior of a periodic composite can be exploited for the optimal design of artificial materials and to explain relevant physiological phenomena, as done for example in [34] in the context of aged bone.

Acknowledgements

This work was supported by the DFG priority program SPP1420, project GE 1894/3 and RA 1380/7, Multiscale structure-functional modeling of musculoskeletal mineralized tissues, PIs Alf Gerisch and Kay Raum. We acknowledge Eli Duenisch for programming support. We are indebted to Alfio Grillo and Sara Tiburtius for insightful discussions and hints about the content of this work.

References

1. Allaire, G.: Homogenization and two-scale convergence. SIAM Journal on Mathematical Analysis **23**(6), 1482–1518 (1992)
2. Auriault, J.L., Boutin, C., Geindreau, C.: Homogenization of coupled phenomena in heterogenous media, vol. 149. John Wiley & Sons (2010)
3. Bakhvalov, N., Panasenko, G.: Homogenisation averaging processes in periodic media. Springer (1989)

4. Boresi, A.P., Chong, K., Lee, J.D.: Elasticity in engineering mechanics. John Wiley & Sons (2010)
5. Bruna, M., Chapman, S.J.: Diffusion in spatial varying porous media. SIAM Journal on Applied Mathematics **75**(4), 1648–1674 (2015)
6. Burridge, R., Keller, J.: Poroelasticity equations derived from microstructure. Journal of acoustical society of America **70**, 1140–1146 (1981)
7. Cherkaev, A., Kohn, R.: Topics in the mathematical modelling of composite materials. Springer (1997)
8. Cioranescu, D., Donato, P.: An Introduction to Homogenization. Oxford University Press (1999)
9. Constantinescu, A., Korsunsky, A.: Elasticity with Mathematica: An Introduction to Continuum Mechanics and Linear Elasticity. Cambridge University Press (2007)
10. Dalwadi, M.P., Griffiths, I.M., Bruna, M.: Understanding how porosity gradients can make a better filter using homogenization theory. In: Proc. R. Soc. A, vol. 471, p. 20150464. The Royal Society (2015)
11. Den Toonder, J., Van Dommelen, J., Baaijens, F.: The relation between single crystal elasticity and the effective elastic behaviour of polycrystalline materials: theory, measurement and computation. Modelling and Simulation in Materials Science and Engineering **7**(6), 909 (1999)
12. Eshelby, J.: The determination of the elastic field of an ellipsoidal inclusion, and related problems. Proceedings of the Royal Society of London. Series A. Mathematical and Physical Sciences **241**, 376–396 (1957)
13. Francfort, G.A., Murat, F.: Homogenization and optimal bounds in linear elasticity. Archive for Rational Mechanics and Analysis **94**(4), 307–334 (1986)
14. Grimal, Q., Raum, K., Gerisch, A., Laugier, P.: A determination of the minimum sizes of representative volume elements for the prediction of cortical bone elastic properties. Biomechanics and Modeling in Mechanobiology **10**(6), 925–937 (2011)
15. Hashin, Z., Shtrikman, S.: A variational approach to the theory of the elastic behaviour of multiphase materials. Journal of the Mechanics and Physics of Solids **11**(2), 127–140 (1963)
16. Hazanov, S.: Hill condition and overall properties of composites. Archive of Applied Mechanics **68**(6), 385–394 (1998)
17. Hill, R.: Elastic properties of reinforced solids: some theoretical principles. Journal of the Mechanics and Physics of Solids **11**(5), 357–372 (1963)
18. Hill, R.: New derivations of some elastic extremum principles. Progress in Applied Mechanics pp. 91–106 (1963)
19. Hill, R.: A self-consistent mechanics of composite materials. Journal of the Mechanics and Physics of Solids **13**(4), 213–222 (1965)
20. Holmes, M.: Introduction to perturbation method. Springer-Verlag (1995)
21. Hori, M., Nemat-Nasser, S.: On two micromechanics theories for determining micro-macro relations in heterogeneous solids. Mechanics of Materials **31**(10), 667–682 (1999)
22. Hull, D., Clyne, T.: An introduction to composite materials. Cambridge university press (1996)
23. Jones, R.M.: Mechanics of composite materials. CRC Press (1998)
24. Kohn, R.V., Lipton, R.: Optimal bounds for the effective energy of a mixture of isotropic, incompressible, elastic materials. Archive for Rational Mechanics

and Analysis **102**(4), 331–350 (1988)
25. Mei, C.C., Vernescu, B.: Homogenization Methods for multiscale mechanics. World Scientific (2010)
26. Milton, G.W.: The theory of composites, vol. 6. Cambridge University Press (2002)
27. Mori, T., Tanaka, K.: Average stress in matrix and average elastic energy of materials with misfitting inclusions. Acta Metallurgica **21**(5), 571–574 (1973)
28. Murat, F.: H-convergence, séminaire danalyse fonctionnelle et numérique (1977/1978). Université dAlger, Multigraphed (1978)
29. Papanicolau, G., Bensoussan, A., Lions, J.L.: Asymptotic analysis for periodic structures. Elsevier (1978)
30. Peerlings, R., Fleck, N.: Computational evaluation of strain gradient elasticity constants. International Journal for Multiscale Computational Engineering **2**(4) (2004)
31. Penta, R., Ambrosi, D., Quarteroni, A.: Multiscale homogenization for fluid and drug transport in vascularized malignant tissues. Mathematical Models and Methods in Applied Sciences **25**(1), 79–108 (2015)
32. Penta, R., Ambrosi, D., Shipley, R.J.: Effective governing equations for poroelastic growing media. The Quarterly Journal of Mechanics and Applied Mathematics **67**(1), 69–91 (2014)
33. Penta, R., Gerisch, A.: Investigation of the potential of asymptotic homogenization for elastic composites via a three-dimensional computational study. Computing and Visualization in Science **17**(4), 185–201 (2016)
34. Penta, R., Raum, K., Grimal, Q., Schrof, S., Gerisch, A.: Can a continuous mineral foam explain the stiffening of aged bone tissue? A micromechanical approach to mineral fusion in musculoskeletal tissues. Bioinspirations and Biomimetics **11**(3), 1–15 (2016)
35. Qu, J.: The effect of slightly weakened interfaces on the overall elastic properties of composite materials. Mechanics of Materials **14**(4), 269–281 (1993)
36. Reuss, A.: Berechnung der Fließgrenze von Mischkristallen auf Grund der Plastizitätsbedingung für Einkristalle. ZAMM - Journal of Applied Mathematics and Mechanics / Zeitschrift fr Angewandte Mathematik und Mechanik **9**(1), 49–58 (1929)
37. Sanchez-Palencia, E.: Non-Homogeneous Media and Vibration Theory-Lecture Notes in Physics 127. Springer-Verlag (1980)
38. Segurado, J., Llorca, J.: A numerical approximation to the elastic properties of sphere-reinforced composites. Journal of the Mechanics and Physics of Solids **50**(10), 2107–2121 (2002)
39. Shipley, R.J., Chapman, J.: Multiscale modelling of fluid and drug transport in vascular tumors. Bulletin of Mathematical Biology. **72**, 1464–1491 (2010)
40. Slawinski, M.A.: Waves and rays in elastic continua. World Scientific (2010)
41. Tartar, L.: Estimation de coefficients homogenises. In: Computing methods in applied sciences and engineering, 1977, I, pp. 364–373. Springer (1979)
42. Tiburtius, S., Schrof, S., Molnár, F., Varga, P., Peyrin, F., Grimal, Q., Raum, K., Gerisch, A.: On the elastic properties of mineralized turkey leg tendon tissue: multiscale model and experiment. Biomechanics and modeling in mechanobiology **13**, 1003–1023 (2014)
43. Voigt, W.: Ueber die Beziehung zwischen den beiden Elasticitätsconstanten isotroper Körper. Annalen der Physik und Chemie, Neue Folge **38**, 573–587

(1888)
44. Zohdi, T.I., Wriggers, P.: An introduction to computational micromechanics, vol. 20. Springer (2008)